Noise and Vibration: *Emerging Methods*
NOVEM 2012
1-4 April 2012 Sorrento

# FREE VIBRATION ANALYSIS OF COMPLEX WING STRUCTURES BY REFINED ONE-DIMENSIONAL FORMULATIONS

E. Carrera , A. Pagani and M. Petrolo

Department of Mechanical and Aerospace Engineering
Politecnico di Torino, Torino, ITALY
Emails: erasmo.carrera@polito.it,
alfonso.pagani@polito.it, marco.petrolo@polito.it

## ABSTRACT

*This paper is focused on the free vibration analysis of aircraft wing models through 1D higher-order models. Refined 1D finite elements were obtained by exploiting the Carrera Unified Formulation (CUF); the 1D models proposed adopt polynomial expansions of the displacement field above the structure cross-section. Two classes of CUF 1D models were developed, the Taylor Expansion models (TE) exploit N-order Taylor-like polynomials, whereas the Lagrange Expansion models (LE) are based on Lagrange polynomials defined on a number of subdomains (L-element) of the cross-section. The order and the type of the cross-section expansion can be arbitrarily chosen since CUF models are hierarchical, that is, the order and the class of the model are input of the analysis. This fundamental capability is obtained by exploiting the fundamental nucleus (FN) of the problem matrices. FN arrays are formally independent of the order and the class of the model. Therefore, stiffness, mass and loading arrays are obtained with no need of ad hoc formulations. CUF 1D models provide 3D-like accuracies with low computational costs for a wide variety of structural configurations, including thin walled structures and composites.*
*In this paper, CUF 1D models were adopted to analyze complex aircraft wings. The typical components of such structures (panels, ribs and stiffeners) were modeled by means of 1D models. The free vibration analysis was conducted and results were compared with solid models by commercial codes. Results highlighted the enhanced capabilities of CUF 1D in terms of implementation ease, high accuracy and low computational costs.*

## 1 INTRODUCTION

Aircraft structures are essentially reinforced thin shells. The so-called *semimonocoque* constructions are composed by three main components: skins (or panels), longitudinal stiffening members and transversal members. Skins have the function to transmit aerodynamic forces and to act with the longitudinal members in resisting the applied loads. Stringers resist bending and axial loads above the skin. Finally, ribs are mainly used to maintain the cross-sectional shape and to redistribute concentrated loads into the structure.
The design of an aircraft wing is a multidisciplinary task and different levels of structural models

are required. In the Finite Element Method (FEM) framework, reinforced-shell structures are generally described as complex systems in which one-dimensional (rod/beam) and two-dimensional (plate/shell) structural elements are properly assembled. A number of works have shown the necessity of a proper simulation of the stiffeners-panel 'linkage' [1–3].
On the other hand, 3D finite element models are usually implemented as soon as wing's structural layouts are determined. Because of their complexity, solid models are commonly used only into optimization procedures. In fact, despite the availabilities of cheaper and cheaper computer power, these FEM models present large computational costs and their use in a multi-field iterative process, such as in an aeroelastic analysis, is quite burdensome.
The present paper proposes a new approach in the analysis of complex wing structures such as reinforced-shell structures. Higher order one-dimensional models, based on the Carrera Unified Formulation (CUF), are used.
CUF 1D models have been recently developed [4] and are based on a hierarchical formulation which considers the order of the theory as an input of the analysis. The finite element formulation is adopted to deal with arbitrary geometries, boundary conditions and loadings.
A number of significant problems dealing with reinforced-shell structures are addressed in the following. The paper is organized as follows: a brief description of the CUF is given in Section 2; numerical results are provided in Section 3; main conclusions are then outlined in Section 4.

## 2 REFINED 1D MODELS

A brief overview on the theoretical model is herein provided. The adopted coordinate frame is presented in Figure 1.

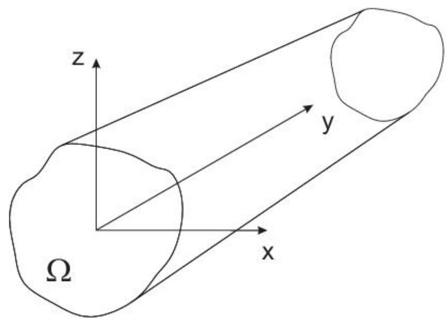


Figure 1. Coordinate frame of the beam model.

The transposed displacement vector is defined as

$$\mathbf{u}(x, y, z; t) = \left\{ \begin{array}{ccc} u_x & u_y & u_z \end{array} \right\}^T \tag{1}$$

Stress, $\boldsymbol{\sigma}$, and strain, $\boldsymbol{\epsilon}$, components are

$$\boldsymbol{\sigma} = \left\{ \begin{array}{cccccc} \sigma_{xx} & \sigma_{yy} & \sigma_{zz} & \sigma_{xy} & \sigma_{xz} & \sigma_{yz} \end{array} \right\}^T, \quad \boldsymbol{\epsilon} = \left\{ \begin{array}{cccccc} \epsilon_{xx} & \epsilon_{yy} & \epsilon_{zz} & \epsilon_{xy} & \epsilon_{xz} & \epsilon_{yz} \end{array} \right\}^T \tag{2}$$

Linear strain-displacement relations are used,

$$\boldsymbol{\epsilon} = \boldsymbol{D}\mathbf{u} \tag{3}$$

where $\boldsymbol{D}$ is a linear differential operator whose explicit expression is not reported here for the sake of brevity, it can be found in [5].
Constitutive laws are exploited to obtain stress components,

$$\boldsymbol{\sigma} = \boldsymbol{C}\boldsymbol{\epsilon} \tag{4}$$

The components of $\boldsymbol{C}$ are the material coefficients. They can be found in [6].

## 2.1 Unified Formulation

In the CUF framework, the displacement field is the expansion of generic functions, $F_\tau$:

$$\mathbf{u} = F_\tau \mathbf{u}_\tau, \qquad \tau = 1, 2, ...., M \tag{5}$$

where $F_\tau$ vary above the cross-section. $\mathbf{u}_\tau$ is the generalized displacement vector and $M$ stands for the number of terms of the expansion. According to the Einstein notation, the repeated subscript, $\tau$, indicates summation. The choice of $F_\tau$ determines the class of 1D CUF model to adopt.
The Taylor Expansion class (TE) is based on Taylor-like polynomial expansions, $x^i\, z^j$, of the displacement field above the cross-section of the structure ($i$ and $j$ are positive integers). The order $N$ of the expansion is arbitrary and is set as an input of the analysis. Static [7, 8] and free-vibration analyses [5, 9] showed the strength of CUF 1D models in dealing with arbitrary geometries, thin-walled structures and local effects. Moreover, asymptotic-like analyses leading to reduced refined models were carried out in [10]. The Euler-Bernoulli (EBBT) and Timoshenko (TBT) classical beam theories are derived from the linear Taylor-type expansion.
The Lagrange Expansion class (LE) exploits Lagrange polynomials to build 1D refined models. Different types of cross-section polynomial sets can be adopted: nine-point elements, L9, four-point elements, L4, etc. LE models have only pure displacement variables. Static analyses on isotropic [11] and composite structures [12] revealed the strength of LE models in dealing with open cross-sections, arbitrary boundary conditions and obtaining Layer-Wise descriptions of the 1D model.
Classical, refined and *component-wise* (CW) models can be implemented by means of CUF 1D. 'Component-wise' means that each typical component of a reinforced-shell structure (i.e. stringers, sheet panels and ribs) can be modeled by means of a unique 1D formulation and, therefore, with no need of ad hoc formulation for each component. This methodology permits us to tune the model capabilities by 1. choosing which component requires a more detailed model; 2. setting the order of the structural model to be used. For more details about CW models see [13, 14].

## 2.2 Finite Element Formulation

The FE approach is herein adopted to discretize the structure along the $y$-axis. This process is conducted via a classical finite element technique, where the displacement vector is given by

$$\mathbf{u}(x, y, z; t) = F_\tau(x, z) N_i(y) \mathbf{q}_{\tau i}(t) \tag{6}$$

$N_i$ stands for the shape functions and $\mathbf{q}_{\tau i}$ for the nodal displacement vector,

$$\mathbf{q}_{\tau i} = \left\{ \begin{array}{ccc} q_{u_{x_{\tau i}}} & q_{u_{y_{\tau i}}} & q_{u_{z_{\tau i}}} \end{array} \right\}^T \tag{7}$$

The explicit forms of the shape functions $N_i$, are not reported here, they can be found in [15].
The stiffness and mass matrices of the elements and the external loadings that are coherent to the models are obtained via the Principle of Virtual Displacements:

$$\delta L_{int} = \delta L_{ext} - \delta L_{ine} \tag{8}$$

where $L_{int}$ stands for the strain energy, $L_{ext}$ is the work of the external loadings, and $L_{ine}$ is the work of the inertial loadings. $\delta$ stands for the virtual variation. The virtual variation of the strain energy and the virtual variation of the work of the inertial loadings can be written as follows:

$$\delta L_{int} = \delta \mathbf{q}_{\tau i}^T \mathbf{K}^{ij\tau s} \mathbf{q}_{sj}, \qquad \delta L_{ine} = \delta \mathbf{q}_{\tau i}^T \mathbf{M}^{ij\tau s} \ddot{\mathbf{q}}_{sj} \tag{9}$$

where $\mathbf{K}^{ij\tau s}$ and $\mathbf{M}^{ij\tau s}$ are the fundamental nuclei of the stiffness matrix and the mass matrix, respectively. The nucleus components of $\mathbf{K}$ and $\mathbf{M}$ do not formally depend on the approximation order. This is the key-point of the CUF which permits, with only nine FORTRAN statements, to implement any-order beam theories. The derivation of the fundamental nuclei is not reported here for the sake of brevity, but it is given in [4, 16], together with a more detailed overview on the CUF. The undamped dynamic problem can be written as

$$\mathbf{M}\ddot{\mathbf{q}} + \mathbf{K}\mathbf{q} = \mathbf{p} \tag{10}$$

where **p** is the loadings vector. Introducing harmonic solutions, it is possible to compute the natural frequencies, $\omega_k$, for the homogenous case, by solving an eigenvalues problem:

$$(-\omega_k^2\mathbf{M} + \mathbf{K})\overline{\mathbf{q}}_k = 0 \tag{11}$$

where $\overline{\mathbf{q}}_k$ is the $k^{th}$ eigenvector.

## 3 NUMERICAL RESULTS

Numerical examples on reinforced-shell wing structures are herein presented. First, static and modal analyzes of a typical aeronautical longeron are considered. Then, the free vibrations analysis of a single-bay box beam is carried out. Solid FE models from the commercial code MSC/NASTRAN® are provided for comparisons. More results can be found in [13, 14].

### 3.1 Longeron

A spar having three longitudinal stiffeners is shown in Figure 2. Stringers are considered rectangular for convenience, anyway they could have whichever shape. The aim of this analysis is to assess a simple structural layout to be exploited for more complex wing structures. The geometrical characteristics are the following: axial length, $L = 3$ $[m]$; cross-section height, $h = 1$ $[m]$; spar caps area, $A_s = 1.6 \times 10^{-3}$ $[m^2]$; sheet panel thickness, $t = 2 \times 10^{-3}$ $[m]$; intermediate stringer's distance from $x$-$y$ plane, $b = 0.18$ $[m]$. The whole structure is made of isotropic material. The material data is: the Young modulus, $E$, is equal to 75 [GPa]; the Poisson ratio, $\nu$, is $0.33$; the density is $\rho = 2.7 \times 10^3$ $[Kg/m^3]$.

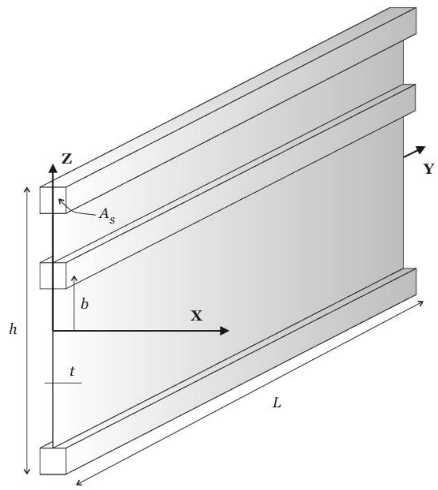


Figure 2. Longeron.

#### 3.1.1 *Static Analysis*

The longeron is clamped at $y = 0$, while a point load, $F_z = -1$ $[N]$, is applied in $[0, L, b]$.
Table 1 shows the vertical displacement, $u_z$, at the loaded point and the number of the degrees of

freedom for each model. A reference solution is obtained according to the following equation:

$$u_{z_{ref}} = \frac{F_z L^3}{3EI} + \frac{F_z L}{AG} \tag{12}$$

Where I is the moment of inertia about $x$-axis, G is the shear modulus and A is the overall cross-section area. A solid FE MSC/NASTRAN® model and classical beam theories are accounted for. The increasing order Taylor-type models are considered in rows $4^{th}$ to $6^{th}$. The LE model is obtained by discretizing the cross-section with 5 L9 elements, one for each spar component (stringers and webs), and the results are shown in the last row.

| | $u_z \times 10^7$ [m] | DOF's |
|---|---|---|
| | $u_{z_{ref}} \times 10^7 = -1.471$ $[m]$ | |
| SOLID | $-1.857$ | 72450 |
| | Classical Beam Theories | |
| EBBT | $-1.325$ | 279 |
| TBT | $-1.487$ | 279 |
| | TE | |
| $N = 4$ | $-1.661$ | 1395 |
| $N = 6$ | $-1.707$ | 2604 |
| $N = 8$ | $-1.730$ | 4185 |
| | LE | |
| 5 L9 | $-1.846$ | 3813 |

Table 1. Displacement values, $u_z$, at the loaded point and number of degrees of freedom.

Figure 3 shows axial stress, $\sigma_{yy}$, and shear stress, $\sigma_{yz}$, trend versus $z$-axis. The SOLID, eighth-order TE and LE models are considered.

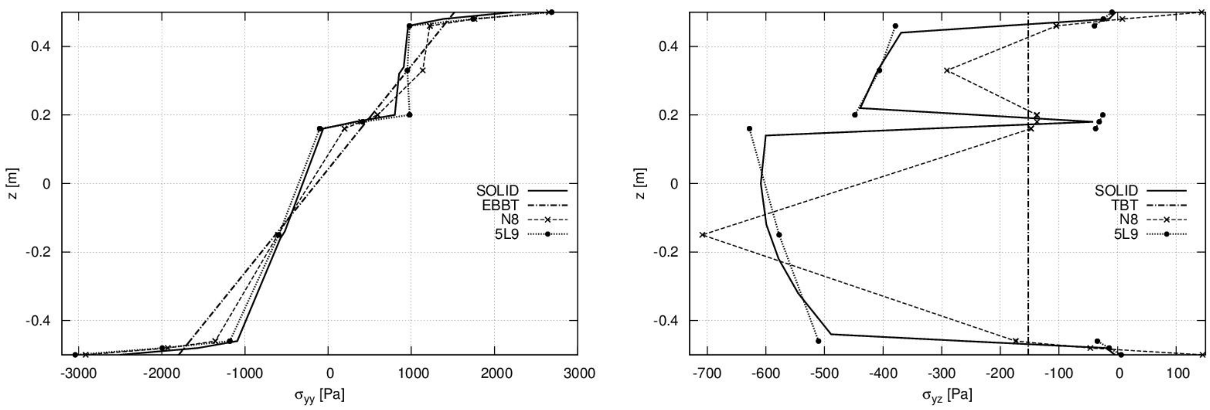


$\sigma_{yy}$ vs. $z$ at $x = y = 0$ $\qquad$ $\sigma_{yz}$ vs. $z$ at $x = 0, y = \frac{L}{2}$

Figure 3. Axial stress, $\sigma_{yy}$, and shear stress, $\sigma_{yz}$, versus $z$-axis, three-stringer spar.

The following statements hold.

- Classical beam theories are not able to correctly predict the mechanical behavior of reinforced-shell structures.
- There is a good agreement between the present refined 1D models and the SOLID model. In particular, the 5 L9 model provide the best accuracy.
- The computational costs of the proposed models are far lower than those required for the SOLID model.

### *3.1.2 Modal Analysis*

A free vibration analysis is carried out. Table 2 shows the natural frequencies of the main modes for each model. The analysis of the results suggest the following comments.

- The classical beam theories and the linear TE model correctly detect first bending and axial modes. No torsional mode is found.
- To correctly predict the torsional modes a higher than second-order TE model is necessary.
- The $5$ L9 model detects the solid FE solution with a significant reduction of the computational cost. Furthermore, local modes are correctly expected by the LE model.

Two modal shapes are drawn. Figure 4 shows the second torsional mode according to the fourth-order TE model, while in Figure 5 a local mode is shown to underline the 3D capabilities of the adopted finite element formulation.

| EBBT | TBT | $N = 2$ | $N = 4$ | 5 L9 | SOLID |
|---|---|---|---|---|---|
| | | I Bending around $z$ | | | |
| $3.24^{(1)*}$ | $3.24^{(1)}$ | $3.43^{(1)}$ | $3.31^{(1)}$ | $3.52^{(2)}$ | $3.55^{(2)}$ |
| | | I Shell-like mode | | | |
| - | - | - | - | $14.27^{(4)}$ | $13.34^{(4)}$ |
| | | I Torsional | | | |
| - | - | $16.70^{(2)}$ | $16.13^{(2)}$ | $16.73^{(5)}$ | $15.06^{(5)}$ |
| | | I Bending around $x$ | | | |
| $117.60^{(5)}$ | $108.81^{(4)}$ | $109.44^{(7)}$ | $102.26^{(7)}$ | $94.75^{(26)}$ | $94.48^{(37)}$ |

$(*)$: in brackets the positions of the frequencies in the eigenvalues vector are reported.

Table 2. Natural frequencies, $[Hz]$, of the main modal shapes.

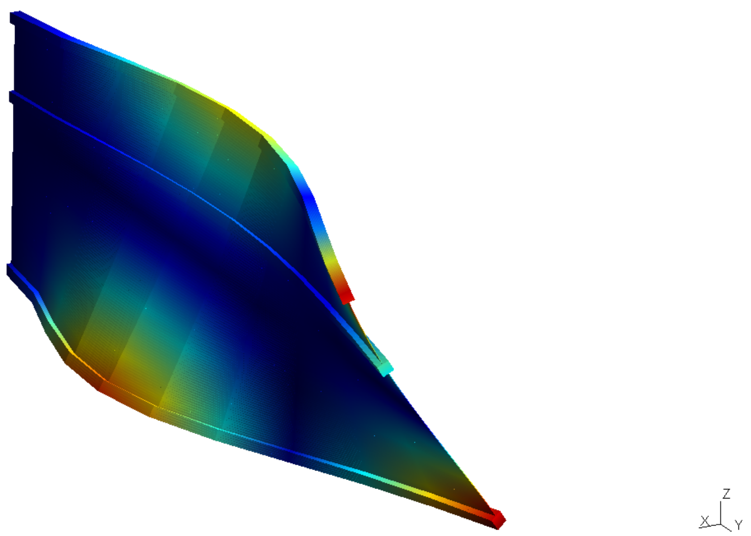


Figure 4. Mode 4, $f_4 = 51.70\ Hz$, fourth-order TE model.

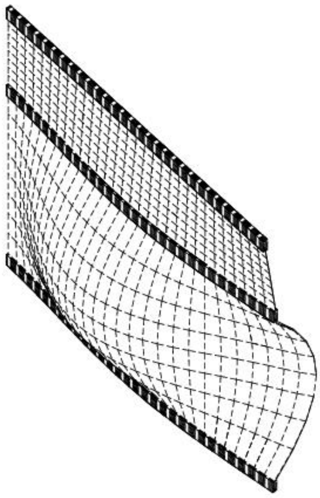

Figure 5. Mode 4, $f_4 = 14.27\ Hz$, LE model.

### 3.2 Free Vibration Analysis of a Wing Box

This section is devoted to the modal analysis of a more complex wing structure. The considered single-bay beam is shown in Figure 6. Two configurations of the same structure are analyzed: a rectangular wing box both with a rib at the tip and without. The aim of this assessment is to underline the capabilities of the present 1D formulation to deal with complex aeronautical structural components. In particular, the following survey wants to highlight the abilities of the CUF 1D to detect ribs and local effects as well as solid and shell-like FEM results.

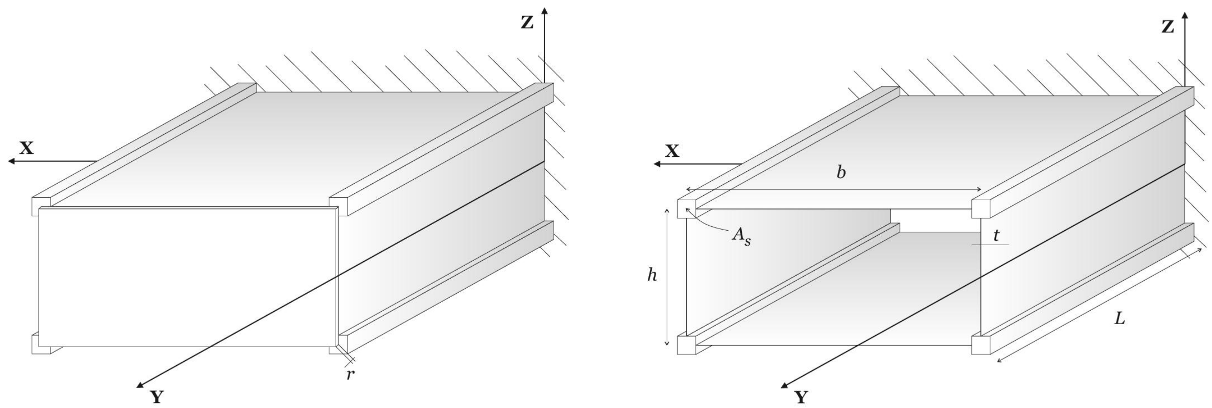


Figure 6. Rectangular wing boxes.

The length-to-width ratio, $L/b$, is equal to $3.125$ with $L$ as high as $3\ [m]$. The cross-section height, $h$, is equal to $0.46\ [m]$, while thickness of the four sheet panels is $t = 2 \times 10^{-3}\ [m]$. The area of the spar caps is $A_s = 1.6 \times 10^{-3}\ [m^2]$. The wing box configuration with a rib at the tip presents a transversal stiffener having a thickness of $r = t$. The structure is made of the same isotropic material of the previous case.
First, let us consider the rectangular wing box with the rib at the tip. Table 3 shows the main natural frequencies and the number of the degrees of freedom for each model. The first column reports the results by EBBT theory. TE models are considered in columns $2^{nd}$ and $3^{rd}$. The LE

model is reported in column $4^{th}$ and it has been implemented by discretizing the cross-section of each component (spar caps, panels, webs) with an L9 element, in order to have an overall mid-span cross-section composed by $8$ L9, while the rib is modeled by means a combination of L4 and L9 elements. Finally, an MSC/NASTRAN® solid model is considered in the last column.

| EBBT | $N = 3$ | $N = 5$ | LE | SOLID |
|---|---|---|---|---|
| | | DOF's | | |
| 306 | 1020 | 2142 | 4860 | 115362 |
| | | I Bending around $x$ | | |
| $67.33^{(1)*}$ | $59.92^{(1)}$ | $58.86^{(1)}$ | $65.39^{(33)}$ | $64.70^{(59)}$ |
| | | I Bending around $z$ | | |
| $127.24^{(2)}$ | $103.64^{(2)}$ | $101.32^{(2)}$ | $105.90^{(45)}$ | $105.57^{(102)}$ |
| | | I Torsional | | |
| - | $223.61^{(3)}$ | $138.18^{(3)}$ | $125.05^{(50)}$ | $131.69^{(135)}$ |
| | | I Differential Bending | | |
| - | - | $467.04^{(9)}$ | $210.36^{(61)}$ | $211.86^{(223)}$ |
| | | I Axial | | |
| $428.48^{(4)}$ | $429.89^{(6)}$ | $417.80^{(8)}$ | $437.23^{(73)}$ | $437.75^{(504)}$ |

$(*)$: in brackets the positions of the frequencies in the eigenvalues vector are reported.

Table 3: Number of the degrees of freedom and natural frequencies, $[Hz]$. Main modal shapes of the ribbed wing box.

The following considerations arise from the analysis.

- Lower-order theories does not take into account the rib deformability, so the differential bending modes are not detected.
- The LE model allow us to obtain solid-like analysis, with a significant improvement in computational costs.

Table 4 shows results by the models of the box with no rib at the tip. Figure 7 shows the differential bending mode, according to the ($N = 7$) TE model.

| EBBT | $N = 3$ | $N = 7$ | 8 L9 | SOLID |
|---|---|---|---|---|
| | | DOF's | | |
| 279 | 930 | 2376 | 4800 | 68304 |
| | | I Differential Bending | | |
| - | - | $63.49^{(3)*}$ | $56.49^{(33)}$ | $57.97^{(57)}$ |
| | | I Bending around $x$ | | |
| $70.57^{(1)}$ | $62.51^{(1)}$ | $60.39^{(2)}$ | $69.99^{(38)}$ | $71.62^{(72)}$ |
| | | I Bending around $z$ | | |
| $133.09^{(2)}$ | $107.72^{(2)}$ | $105.01^{(5)}$ | $111.20^{(53)}$ | $109.20^{(109)}$ |
| | | I Torsional | | |
| - | $224.50^{(3)}$ | $166.67^{(8)}$ | $153.53^{(60)}$ | $160.02^{(176)}$ |
| | | I Axial | | |
| $439.21^{(4)}$ | $441.04^{(6)}$ | $440.41^{(29)}$ | $440.49^{(88)}$ | $437.63^{(498)}$ |

$(*)$: in brackets the positions of the frequencies in the eigenvalues vector are reported.

Table 4: Number of the degrees of freedom and natural frequencies, $[Hz]$. Main modal shapes of the rib-free wing box.

The conducted analysis highlights the following comments.

- The LE model and the higher than seventh-order TE models correctly foresee the lack of the rib at the tip, according to the SOLID model.
- Once again, the LE model returns the best 'computational costs/accuracy' ratio.

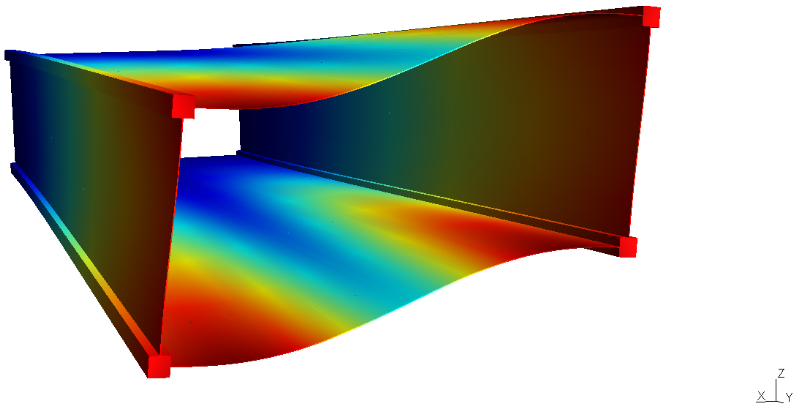


Figure 7. Mode 3, $f_3 = 63.49\ Hz$, seventh-order TE model.

## 4 CONCLUSIONS

Two structural problems have been discussed in this paper, including longerons and single-bay box beams. Comparisons with solid models from commercial codes were provided. The results obtained suggest the following.

- The proposed refined 1D models offer a good accuracy in detecting the mechanical behavior of wing structures. In particular, torsional, differential bending and shell-like modes are foreseen by opportunely increasing the order of the model.
- The capability offered by the CUF 1D models of detecting ribs and local effects allows us to deal with a large variety of complex wing structures, such as in [13, 14], where the LE models are exploited in a CW approach to model multi-bay box beams.
- The present formulation is extremely convenient in terms of computational costs if compared to solid models. This aspect is of fundamental importance, since the design of a wing involves coupled problems (fluid-structure interaction) and it is often an iterative process.

Future investigations should deal with the implementation of the spectral analysis to the higher-order 1D elements. It should improve the prediction of the dynamic characteristics of the structure, since the finite element solution become increasingly inaccurate as the frequency increases.

## REFERENCES


[1] G. M. Vörös. A special purpose element for shell-beam systems. *Computers and Structures*, 29(2):301–308, 1988.

[2] M. Kolli and K. Chandrashekhara. Finite element analysis of stiffened laminated plates under transverse loading. *Composite Science and Technology*, 56:1355–1361, 1996.

[3] S. N. Patel, P. K. Datta, and A. H. Seikh. Buckling and dynamic instability analysis of stiffened shell panels. *Thin-Walled Structures*, 44:321–333, 2006.

[4] E. Carrera, G. Giunta, and M. Petrolo. *Beam Structures: Classical and Advanced Theories*. John Wiley & Sons, 2011. DOI: 10.1002/9781119978565.

[5] E. Carrera, M. Petrolo, and P. Nali. Unified formulation applied to free vibrations finite element analysis of beams with arbitrary section. *Shock and Vibrations*, 18(3):485–502, 2011. DOI: 10.3233/SAV-2010-0528.

[6] J. N. Reddy. *Mechanics of laminated composite plates and shells. Theory and Analysis*. CRC Press, $2^{nd}$ edition, 2004.

[7] E. Carrera, G. Giunta, P. Nali, and M. Petrolo. Refined beam elements with arbitrary cross-section geometries. *Computers and Structures*, 88(5–6):283–293, 2010. DOI: 10.1016/j.compstruc.2009.11.002.

[8] E. Carrera, G. Giunta, and M. Petrolo. *A Modern and Compact Way to Formulate Classical and Advanced Beam Theories*, chapter 4, pages 75–112. Saxe-Coburg Publications, Stirlingshire, UK, 2010. DOI: 10.4203/csets.25.4.

[9] E. Carrera, M. Petrolo, and A. Varello. Advanced beam formulations for free vibration analysis of conventional and joined wings. *Journal of Aerospace Engineering*, 2011. In Press.

[10] E. Carrera and M. Petrolo. On the effectiveness of higher-order terms in refined beam theories. *Journal of Applied Mechanics*, 78(3), 2011. DOI: 10.1115/1.4002207.

[11] E. Carrera and M. Petrolo. Refined beam elements with only displacement variables and plate/shell capabilities. *Meccanica*, 47(3):537–556, 2012. DOI: 10.1007/s11012-011-9466-5.

[12] E. Carrera and M. Petrolo. A beam formulation with shell capabilities. In *Proceedings of 51st AIAA/ASME/ASCE/AHS/ASC Structures, Structural Dynamics, and Materials Conference*, Orlando, Florida, USA, April 2010.

[13] E. Carrera, A. Pagani, and M. Petrolo. Classical, refined and component-wise theories for static analysis of reinforced-shell wing structures. 2012. To be Submitted.

[14] E. Carrera, A. Pagani, and M. Petrolo. Component-wise method applied to vibration of wing structures. 2012. To be Submitted.

[15] K. J. Bathe. *Finite element procedure*. Prentice hall, 1996.

[16] E. Carrera and G. Giunta. Refined beam theories based on a unified formulation. *International Journal of Applied Mechanics*, 2(1):117–143, 2010. DOI: 10.1142/S1758825110000500.